

# LTE-Advanced Radio and Network Optimization: Basic Coverage and Interference Constraints

Fernando J. Velez<sup>1,2</sup>, Sofia Sousa<sup>1</sup>, Jessica Acevedo Flores<sup>1</sup> and Daniel Robalo<sup>1</sup>

<sup>1</sup>Instituto das Telecomunicações - DEM  
Universidade da Beira Interior, Faculdade de Engenharia  
6201-001 Covilhã, Portugal  
fjv@ubi.pt, sofia.sousa@lx.it.pt, {jessik1512,  
robalodaniel}@gmail.com

Albena Mihovska and Ramjee Prasad  
<sup>2</sup>Center for TeleInfrastruktur (CTIF)  
Department of Electronic Systems  
Aalborg University  
9220 Aalborg, Denmark  
albena@es.aau.dk, prasad@es.aau.dk

**Abstract**—In cellular optimization, the UL and DL the values from carrier-to-noise-plus-interference ratio (CNIR) from/at the mobile station are very important parameters. From a detailed analysis of its variation with the coverage and reuse distances for different values of the Channel Quality Indicator (CQI) and given ITU-R propagation models, an evaluation of the possible range for the reuse factor of LTE-A is performed for the DL. By considering CQI and reference CNIR requirements recommended by 3GPP, DL peak bit rates along with the Transport Block Size assumed for single stream and bandwidths of 10 and 20 MHz, PHY and supported throughputs are analysed. HetNets with Carrier Aggregation are considered, where macro cells operating at 800 MHz provide coverage and small cells (SCs) operating at 2.6 GHz provide throughput enhancement at hotspots. A clear decrease is shown for the supported throughput for the longest coverage distances in NLoS propagation conditions. In the given range of coverage distances, the same maximum value occurs for the supported throughput for  $K=3$  and 7, both for macro and SCs.

**Keywords**—LTE-Advanced; CNIR; ITU-R propagation model; radio and network optimization; system capacity; HetNet

## I. INTRODUCTION

In nowadays wireless cellular networks, not only mobile services and applications usage is increasing each year, leading to an expansion of mobile data traffic, but the pace at which it is growing is accelerating. According to [1], in 2013 mobile data traffic was nearly 18 times the size of the entire global Internet in 2000. One Exabyte of traffic traversed the global Internet in 2000, and in 2013 mobile networks carried nearly 18 Exabyte's of traffic. In 2013 alone, 526 million mobile devices and connections were added, the global mobile data traffic grew 81 % and mobile video represented 53 % of all mobile traffic and by 2018 it will reach 69 %. Moreover, mobile-connected devices exceed the world's population by 2014. Monthly mobile data traffic will reach 15.9 Exabyte's by 2018 and between 2013 and 2018 the annual growth rate is 61 %, i.e., mobile data traffic will increase nearly 11-fold between 2013 and 2018. These statistics show beyond the shadow of a doubt that wireless and cellular networks technologies need to be enhanced to support such demands. As such, this paper gives contributions to the basic limits of the optimization and planning of 4G cellular networks in a context of heterogeneous (HetNets) Long Term Evolution - Advanced (LTE-A) and spectrum management. LTE-A provides seamless Internet Protocol (IP) connectivity between user equipment (UE) and the packet data network (PDN), and an air

interface based on Orthogonal Frequency Division Multiplexing (OFDM) in the downlink (DL) and single-carrier frequency-division multiple access (SC-FDMA) in the uplink (UL), both providing high flexibility in the frequency-domain scheduling. LTE-A has the flexibility to support time-/frequency-division duplexing (TDD/FDD) and half-duplex FDD schemes.

The main goal of cellular coverage is to offer access to mobile users in a cell, while guaranteeing quality of the received signal in both DL and UL directions, even for the users at the cell edge. As resources, e.g., radio frequency channels, need to be reused in different geographical zones (but not in the closest proximity), the impact of interference among co-channel cells needs to be evaluated in both DL e UL directions. Furthermore, this interference is heavier in users at cell edge, who may suffer from low connection quality. Therefore, a comprehensive study on the variation of the UL/DL carrier-to-noise-plus-interference ratio (CNIR) from/at the Mobile Station (MS) with different system parameters is critical in the context of LTE-A optimization. In this work, we are just considering DL. The variation of CNIR with the coverage and reuse distances is analysed for different values of the Channel Quality Indicator (CQI) and respective Modulation and Coding Scheme (MCS), considering the macro and pico cellular layers from a HetNet.

OFDM is a digital multi-carrier modulation scheme that extends the concept of single subcarrier modulation by using multiple subcarriers within the same single channel. Rather than transmit a high-rate stream of data with a single subcarrier, OFDM makes use of a large number of closely spaced orthogonal subcarriers that are transmitted in parallel. Each subcarrier is modulated with a conventional digital modulation scheme (such as QPSK, 16QAM, 64QAM.) at low symbol rate.

The goal of considering adaptive modulation is to choose the appropriate MCS for transmission in each carrier, given the local CNIR [2]. The MCS is chosen from an LTE-specific look-up table according to the provided Channel Quality Indicator (CQI) feedback [3]. The corresponding MCS value should achieve the maximum possible throughput by guaranteeing that the Block Error Ratio (BLER) is a bellow a given threshold.

Table I shows the mapping established with the MCS index and reference CNIR requirements recommended by 3GPP for DL, Los/NLoS as well as the spectral efficiency,  $S_{eff}$ . Table II presents DL peak bit rates,  $R_p$ , considered for single stream and bandwidth of 10 and 20 MHz.

TABLE I. MINIMUM CNIR, MODULATION AND SPECTRAL EFFICIENCY VERSUS MCS, FOR LTE, AND VALUES FOR THE VERTICAL ASYMPTOTE FOR DL

MCS mapping			$R_{\text{asymptote}} [\text{km}]$						$R_b [\text{Mbps}]$	
Mod. index	$\text{CNIR}_{\text{min}} [\text{dB}]$	Modulation	ITBS	$S_{\text{off}}$	$f = 800 \text{ MHz, macro}$			$f = 2.6 \text{ GHz, pico}$		$\frac{R_b}{BW}$
					10 MHz	10 MHz NLoS	10 MHz	10 MHz NLoS	20 MHz NLoS	
1	-4.63	QPSK	0	0.23	28.922	9.251	4.666	1.009	0.836	1.384
2	-3.615		1	0.31	27.281	8.714	4.401	0.947	0.784	1.8
3	-2.6		2	0.38	25.732	8.208	4.151	0.889	0.736	2.216
4	-1.36		3	0.49	23.959	7.630	3.865	0.822	0.681	2.856
5	-0.12		4	0.6	22.309	7.092	3.599	0.761	0.630	3.624
6	1.17		5	0.74	20.712	6.573	3.342	0.702	0.581	4.392
7	2.26		6	0.88	19.453	6.164	3.138	0.655	0.542	5.16
8	3.595		7	1.03	18.014	5.698	2.906	0.603	0.499	6.2
9	4.73		8	1.18	16.874	5.330	2.722	0.561	0.465	6.968
10	6.13	9	1.33	15.568	4.908	2.512	0.514	0.425	7.992	
11	7.53	16-QAM	9	1.33	14.362	4.519	2.317	0.471	0.390	7.992
12	8.1		10	1.48	13.899	4.370	2.242	0.454	0.376	8.76
13	8.67		11	1.7	13.450	4.226	2.170	0.438	0.363	9.912
14	9.995		12	1.91	12.462	3.908	2.011	0.403	0.334	11.448
15	11.32		13	2.16	11.547	3.615	1.863	0.371	0.307	12.96
16	12.78		14	2.41	10.616	3.317	1.713	0.339	0.280	14.112
17	14.24		15	2.57	9.761	3.044	1.575	0.309	0.256	15.264
18	14.725		15	2.57	9.492	2.958	1.531	0.300	0.248	15.264
19	15.21		16	2.73	9.231	2.875	1.489	0.291	0.241	16.416
20	16.92	64-QAM	17	3.03	8.365	2.599	1.350	0.261	0.216	18.336
21	18.63		18	3.32	7.581	2.350	1.223	0.235	0.194	19.848
22	19.975		19	3.61	7.016	2.171	1.132	0.216	0.178	21.384
23	21.32		20	3.9	6.493	2.006	1.048	0.198	0.164	22.92
24	22.395		21	4.21	6.104	1.883	0.985	0.185	0.153	25.456
25	23.47		22	4.52	5.738	1.767	0.926	0.173	0.143	27.376
26	25.98		23	4.82	4.966	1.524	0.801	0.148	0.122	28.336
27	28.49		24	5.12	4.298	1.315	0.693	0.126	0.105	30.576
28	31.545		25	5.33	3.605	1.098	0.582	0.104	0.086	31.704
29	34.6	26	5.55	3.023	0.917	0.488	0.086	0.071	36.696	

TABLE II. DL PEAK BIT RATES AND MINIMUM CNIR FOR BANDWIDTH OF 5 MHz, 10 MHz AND 20 MHz - 25, 50 & 100 RESOURCE BLOCKS RESPECTIVELY

Modulation	$\text{CNIR}_{\text{min}} [\text{dB}]$	$R_p [\text{Mbps}]$ , 5 MHz	$R_p [\text{Mbps}]$ , 10 MHz	$R_p [\text{Mbps}]$ , 20 MHz
QPSK/16-QAM/64-QAM	-4.63/7.53/14.725	4/7.7/18.3	7.9/15.3/36.7	15.8/30.5/75.4

Power and gains assumed in the considered LTE scenario are presented in Table III for 800 MHz/2.6 GHz LTE.

TABLE III. POWER, GAIN AND NOISE PARAMETERS

Parameters	$f [\text{GHz}]$	$P_t [\text{dBW}]$	$G_t [\text{dBi}]$	$G_r [\text{dBi}]$	$BW [\text{MHz}]$	$N_f [\text{dB}]$
Macro/Pico	0.8 / 2.6	16 / -7	17	0	10 / 20	5

The remainder of the paper is organized as follows. Section II addresses the interference, noise and frequency reuse trade-offs involved in LTE radio and HetNet optimization considering different MCSs, LoS versus NLoS propagation, comparing the behaviour of the 800 MHz and 2.6 GHz frequency bands (macro/pico cellular layers, respectively) whilst briefly mentioning the analytical formulations. Section III presents a detailed analysis of LTE system capacity considering assumptions for different levels of MCSs, and discusses original results for the equivalent supported throughput as a function of the coverage distance. Finally, conclusions are drawn in Section IV.

## II. CELLULAR RADIO AND HETNET OPTIMIZATION

In HetNets, cellular radio/network optimization must consider interference in obtaining the maximum coverage distance since it is a critical limitation in cellular systems dimensioning process. Noise is also an essential factor for the interference analysis, since it is always present in communications. Therefore, cellular optimization has to simultaneously consider carrier-to-noise and carrier-to-interference constraints. This work evaluates a 3GPP Carrier Aggregation (CA) scenario [4]. This scenario allows a flexible use of fragmented spectrum in different frequency bands. A lower frequency, 800 MHz, at the macro base station (eNB) layer provides coverage while the 2.6 GHz frequency band, at a pico-cell layer, improves throughput at hot spots. Mobility

through CA is performed based on the macro eNB. The work considers LoS and NLoS propagation. Given the future reality in Portugal and Europe, the values for the evaluated bandwidth,  $BW$ , are 10 and 20 MHz both for the 800 MHz and 2.6 GHz frequency bands. The cell range at macro cellular layer varies from 150 to 3000 m, except in one example, while for small cells it varies from 25 to 300 m.

In order to select the appropriate reuse pattern,  $K$ , and the appropriate frequency band, radio and network optimization aspects, like the analysis of cell coverage distance (or cell radius), co-channel reuse factor (ratio between the reuse and coverage distances),  $K$ , and supported throughput are addressed in this work for several levels of LTE MCS.

### A. Analytical Formulations

If one considers the interference-to-noise ratio,  $M$ , defined by the ratio between the interference and noise powers,  $M=I/N$ , and the equation for the carrier-to-noise-plus-interference ratio (CNIR) to be used in the dimensioning process is the following:

$$\left(\frac{C}{N+I}\right) = \left(\frac{C}{N}\right)_{\text{min}} \quad (1)$$

equation (1) can be re-written in the two following ways:

$$\left(\frac{C}{N}\right) = \left(\frac{C}{N}\right)_{\text{min}} (1 + M) \quad (2)$$

$$\left(\frac{C}{I}\right) = \left(\frac{C}{N}\right)_{\text{min}} (1 + M^{-1}) \quad (3)$$

In (1) one is considering the model for CNIR from [5] while assuming that weights for noise and interference are the same.

The interference-to-noise ratio is defined by

$$M(R) = \left(\frac{C(R)}{N}\right) - 1 \quad (4)$$

where  $C(R)=P_R(R)$  is computed by applying, e.g., the ITU-R propagation model from [6]. Values of  $M(R)$  are proportional to interference still tolerable for a given coverage distance,  $R$ , while (still) agreeing with the quality requirements for a given MCS.

With hexagonal cell topologies for the macro and pico cellular layers, in the DL, as shown in Figure 1,  $C/I$  is given by:

$$\frac{C}{I} = \frac{1}{2(r_{cc}+1)^{-\gamma} + 2r_{cc}^{-\gamma} + 2(r_{cc}-1)^{-\gamma}} \approx \frac{r_{cc}^{\gamma}}{6} \quad (5)$$

where  $r_{cc}$  is the co-channel reuse factor, given by  $r_{cc}=D/R$ ,  $D$  is the reuse distance and  $R$  is the coverage distance (N.B. different  $D_s$  and  $R_s$  are defined for the macro and pico- cellular layers). In dB, the approximate equation is therefore  $C/I \approx 10 \cdot \gamma \log_{10}(r_{cc}/6)$ . By replacing (5) into (3), it is possible to obtain the following equation for the reuse factor in the DL:

$$r_{cc} = \sqrt[3]{6 \cdot (1 + M^{-1}) \cdot (C/N)_{\text{min}}} \quad (6)$$

As a horizontal asymptote arises in the analysis of the curves of  $r_{cc}$  as a function of the coverage distance,  $R$ , it is important to present the mathematical details associated to it. To compute the horizontal asymptote in the chart from  $r_{cc}(R)$ , one has to consider that  $R \rightarrow 0$ . Note that reuse pattern is given by  $K=r_{cc}^2/3$ .

From equation (6), if  $R \rightarrow 0$  then  $M \rightarrow +\infty$ , and  $M^{-1} \rightarrow 0$ . For the DL, in the limit, one obtains:

$$\lim_{R \rightarrow 0} r_{cc} = \sqrt[3]{6 \cdot (C/N)_{\text{min}}} \quad (7)$$

By considering the dependence of  $K$  on  $r_{cc}$ , it is straightforward to conclude that, for each value for the propagation exponent, apart from the dependence on the cellular interference geometry,  $K$  only depends on MCS through the corresponding minimum carrier-to-noise ratio.

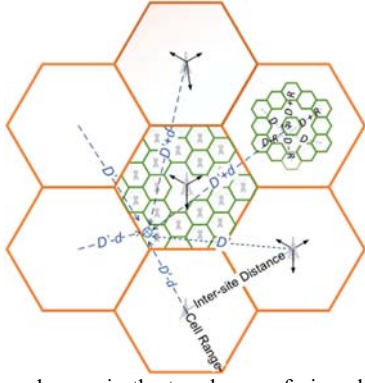


Fig. 1. Coverage and reuse in the two layers of pico plus macro HetNet, where co-channel interference is represented in the worst-case for the DL.

While the asymptotic reuse factor,  $r_{cc}$ , is associated with the upper bound for system capacity, the maximum coverage distance is associated with the carrier-to-interference-plus-noise ratio at the cell boundary when the interference is null. The vertical asymptote,  $R_{asymptote}$ , from  $M(R)$  and  $r_{cc}(R)$  represents the interference that can still be tolerated for a given  $R$ , in the limit, the maximum coverage distance for which no extra interference is tolerated.

### B. Interference-to-noise Ratio and Co-channel Reuse Factor

By considering  $R_{asymptote} = R_{M \rightarrow 0}$ , one obtains the curves for the DL interference-to-noise ratio, considering the macro and micro/picocellular scenarios from ITU-R model [6] for the 800 MHz and 2.6 GHz frequency bands, respectively. For the micro/picocellular scenario, the considered height from the macro base station is  $h_{BS} = 10$  m. For the macrocellular scenario, the height of the macro eNB is 25 m. The height of the mobile user is always  $h_{UT} = 1.5$  m. Variables  $h'_{BS[m]} = h_{BS} - 1$  and  $h'_{UT[m]} = h_{UT} - 1$  also stand. At 800 MHz, the breakpoint distance is  $d_{BP} = 4 \cdot 24 \cdot 0.5 \cdot 800 \cdot 10^6 / c = 128$  m, where  $c$  is the velocity of the light. For the 2.6 GHz frequency band,  $d_{BP} = 4 \cdot 9 \cdot 0.5 \cdot 2.6 \cdot 10^9 / c = 156$  m. By considering these assumptions, in LoS, at 800 MHz, the path loss, PL, in dB is given by:  $PL(d) = 22.0 \cdot \log_{10}(d_{[m]}) + 26.0618$ , for  $d < 128$  m, and  $PL(d) = 40 \cdot \log_{10}(d_{[m]}) - 11.819$ , for  $d \geq 128$  m. Also in LoS, at 2.6 GHz, for  $d < 156$  m,  $PL(d) = 22.0 \cdot \log_{10}(d_{[m]}) + 36.29947$ , while for  $d \geq 156$  m one achieves  $PL(d) = 40 \cdot \log_{10}(d_{[m]}) - 3.12788$ . In NLoS, the considered street width considered is 20 m while the average building height is 20 m. In the NLoS PL model there is no breakpoint. At 800 MHz,  $PL(d) = 39.08639 \cdot \log_{10}(d_{[m]}) + 11.6067$  while at 2.6 GHz one achieves  $PL(d) = 36.7 \cdot \log_{10}(d_{[m]}) + 33.48$ .

Considering the values for  $P_t$ ,  $G_t$ ,  $G_r$ ,  $BW$  and  $N_f$  from Table III, we obtained values for interference-to-noise-ratio,  $M$ , in the DL for  $f = 800$  MHz.  $M(R)$  depends on the CQI value and the MCS associated to it. Apart from the mapping between the MCS index and minimum CNIR,  $CNIR_{min}$ , Table I presents the corresponding values for the vertical asymptote,  $R_{asymptote}$ , for macro cells operating at 800 MHz and for pico cells operating at 2.6 GHz (LoS/NLoS). At 800 MHz, one only discusses results  $BW = 10$  MHz, as the distances for the vertical asymptotes for  $BW = 20$  MHz are only slightly shorter. However, for the 2.6 GHz case, one also addresses results for  $BW = 20$  MHz. A relevant decrease of the values for the vertical asymptote (maximum  $R$ ) occurs as the MCS increases because of the lowest associated  $CNIR_{min}$ .

Charts for the interference-to-noise ratio,  $M(R)$ , and reuse factor,  $r_{cc}$ , are shown in Figures 2-3 for the 800 MHz frequency band ( $0 \leq R \leq 3000$  m) for  $BW = 10$  MHz. Values from  $r_{cc}$  span from circa 1 up to 12 while the MCS order increases. Although charts for  $BW = 20$  MHz are not presented here, values of  $M$  are slightly lower than for  $BW = 10$  MHz, because of the highest noise power. Consequently,  $R_s$  for the vertical asymptotes are slightly shorter for  $BW = 20$  MHz. The chart of  $r_{cc}$  is also not presented because, apart from the shortest  $R_s$  for the asymptotes, the results for  $BW = 20$  MHz are very similar to the ones from Figure 3. From this analyses it is possible to conclude that the highest order MCSs can only be supported with high  $r_{cc}$  (hence high  $K$ ).

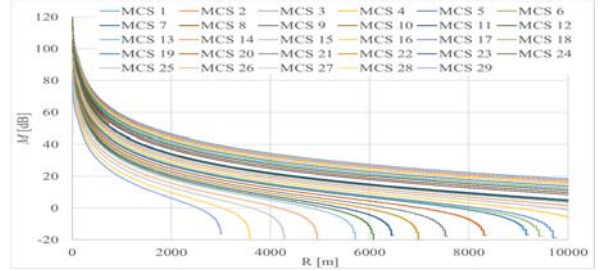


Fig. 2 Interference to noise ratio as a function of the coverage distance with MCS as a parameter for DL, in the 800 MHz band,  $BW = 10$  MHz.

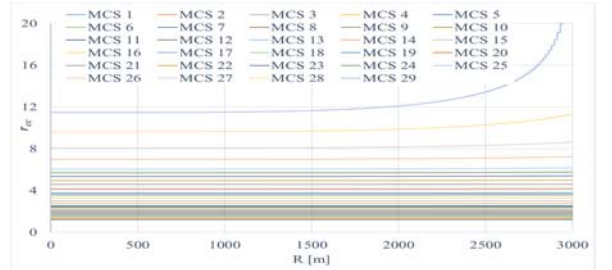


Fig. 3 Co-channel reuse factor as a function of the coverage distance with MCS as a parameter for DL, in the 800 MHz band, LoS,  $BW = 10$  MHz.

Figures 4-5 analyse the case of 800 MHz band, NLoS,  $BW = 10$  MHz. The vertical asymptotes are clearly shorter. However, as the propagation exponent is 3.909, instead of 4, the behaviour of  $r_{cc}$  for the shortest distances is similar to the one from LoS case. Figure 6 presents the variation of  $M(R)$  for the pico cellular layer, 2.6 GHz-LoS. The breakpoint is clearly visible for  $R = 156$  m. The shortest  $R$  for the vertical asymptotes occurs for  $R = 488$  m (MCS 29); hence, no vertical asymptote is visible for  $R_s$  up to 300 m. Although the chart for  $r_{cc}$  is not presented here, the horizontal asymptotes for  $r_{cc}$  are the same as for the 800 MHz band, LoS, as the propagation exponent is also  $\gamma = 4$ . For  $BW = 20$  MHz,  $M$  is slightly lower (resulting in shorter asymptotes).

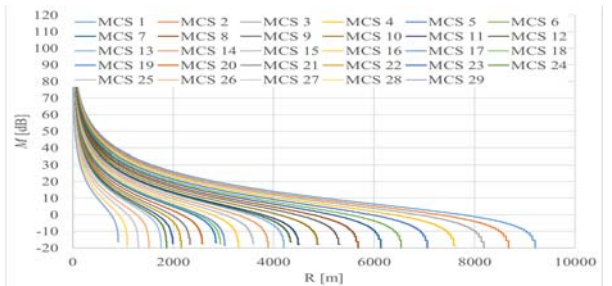


Fig. 4 Interference to noise ratio as a function of  $R$  with MCS as a parameter for DL, in the 800 MHz band, NLoS,  $BW = 10$  MHz.

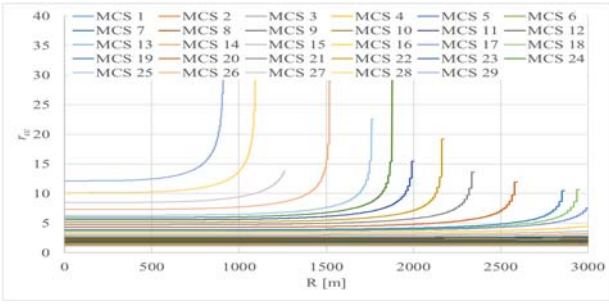


Fig. 5 Co-channel reuse factor as a function of the coverage distance with MCS as a parameter for DL, in the 800 MHz band, NLoS,  $BW = 10$  MHz.

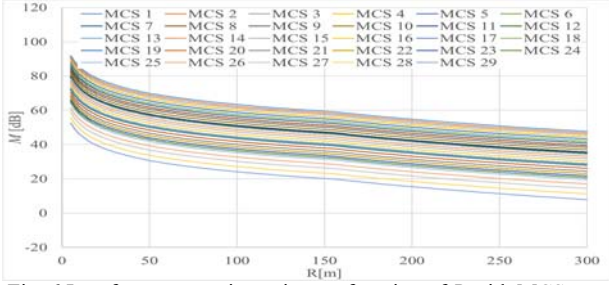


Fig. 6 Interference to noise ratio as a function of  $R$  with MCS as a parameter for DL, in the 2.6 GHz band, LoS,  $BW = 10$  MHz.

In the case of 2.6 GHz-NLoS, the propagation exponent is  $\gamma=3.67$  and the path loss additive constant is higher than before.  $M$  is lower, and the asymptotes become visible in the range of  $R$ s up to 300 m. Besides, an increase in  $r_{cc}$  exists. There are limitations in the coverage with the highest MCSs for the shortest  $R$ s. For  $BW=20$  MHz vertical asymptotes are slightly shorter compared to  $BW=10$  MHz, resulting in worst coverage for short distances.

### C. CNIR as a Function of $r_{cc}$ with $R$ as Parameter

Figure 7 facilitates to analyse the variation of the CNIR with  $r_{cc}$ , with  $R$  as parameter. Different frequency bands are considered as well as LoS versus NLoS propagation. When the interference power is much higher than noise power, the CNIR is given simply by  $C/I \approx r_{cc}^\gamma/6$  in linear terms. In the analysis from Figure 7, this occurs in the majority of the cases, as interference,  $I$ , is always much higher than noise,  $N$ , i.e.,  $M > 8-10$  dB, except for the cases “2.6 GHz-NLoS- $R=300$  m” and “800 MHz-NLoS- $R=750$  m”, where  $M < 8$  dB for  $r_{cc} \geq 2.85$  and  $r_{cc} \geq 8.75$ , respectively. Hence, in the general case, the curves just follow the trend  $10 \cdot \gamma \log_{10}(r_{cc}/6)$ . From propagation models, one can observe that  $\gamma$  varies from 3.67 to 4, except for distances below the breakpoint. The exception occurs in the “2.6 GHz-LoS- $R=15$  m” case (blue curve). In the “2.6 GHz-LoS- $R=15$  m” case, for the purpose of  $C/I$  computation, the value of  $\gamma$  is 2.2 (the lowest  $\gamma$  in our analysis).

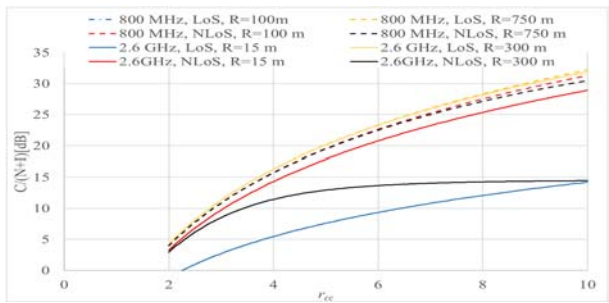


Fig. 7 Variation of the CNIR with  $r_{cc}$  for the DL in the 800 MHz and 2.6 GHz frequency band, LoS versus NLoS, and  $BW=10$  MHz.

Also in the “800 MHz-LoS- $R=100$  m” case,  $\gamma$  is considered to be 2.2 – but just for coverage purposes. When the system is noise limited (clearly the case “2.6 GHz-NLoS- $R=300$  m” for  $r_{cc} \geq 2.85$ , black dashed curve)  $CNIR(r_{cc})$  follows a trend different from the one represented by  $C/I \approx r_{cc}^\gamma/6$ . Furthermore, if  $R$  increases for several hundreds of meters or even some kilometres, the reuse distance ( $D=r_{cc}R$ ), considered in the computation of interference, considerably increases and interference decreases. Interference becomes comparable to (not much higher than) noise. Hence, the curves of CNIR become lower than the upper limit curve. It is also a worth mentioning that the mapping between these values of CNIR and  $R_b$  are obtained by considering the correspondence from Table I (or Table II, in a simpler approach).

### III. DETAILED ANALYSIS OF SYSTEM CAPACITY

While previous Sections analysed the individual influence of each MCS, it is also worthwhile to study the overall impact of several MCSs. Following the formulation from [7] for an implicit function procedure to compute supported throughput, the LTE system capacity is analysed for both macro (800 MHz) and pico (2.6 GHz) cellular layers from a Hetnet, considering the ITU-R propagation model [6]. The analysis considers different values of the reuse pattern, e.g.,  $K=1, 3$  and  $7$ . One considers the values for  $P_t, G_t, G_r, BW$  and  $N_f$  from Table III. To map  $CNIR_{min}$  into supported throughput one has assumed the values from  $CNIR_{min}$  provided by [3], more specifically Tables 7.1.7.1-1 and 7.1.7.2.1-1. By extrapolating the gathered information it is possible to map the CNIR into MCS index, Modulation Order Transport Block Size (ITBS) index and TBS. Furthermore, by assuming  $TTI=1$  ms the PHY throughput is obtained by multiplying the TBS by this value, and e.g., if 5 MHz bandwidth is considered, i.e., 25 PRBs, column NPRB=25 from Table 7.1.7.2.1-1 from [3] is assumed. This relation is presented in p. 122 from [7] (for  $BW=5$  MHz), and in the last column from Table I (for  $BW=10$  MHz), and similar relation exists for  $BW$  of 20 MHz. The maximum achievable number of coverage rings and MCSs are equal, i.e., 29, as each corresponds to different value of the PHY throughput. Figures 8 and 9 analyse the variation of CNIR and  $R_b$  with the distance  $d$  from cell centre to UE within a cell, where  $0 \leq d \leq R$ , as shown in Figure 1. Respective cell sizes are  $R=3000$  and  $300$  m, at 800 MHz and 2.6 GHz, respectively, for  $BW=10$  MHz,  $K=7; 3$ . In “NLoS”, CNIR and throughput are clearly lower than in “LoS”. For the macro cellular layer, the curve for CNIR for  $K=3$  ( $r_{cc}=3$ ) is clearly lower than for  $K=7$  ( $r_{cc}=4.58$ ) because of the much higher interference, resulting from the shortest  $D$ . This is evident both considering the LoS or NLoS propagation. For the macro cellular layer the curve for CNIR in the NLoS propagation is clearly lower than for the pico cellular layer. For both (pico and macro) scenarios, by considering the mapping between  $CNIR_{min}$  and  $R_b$  we clearly observe that the stepwise throughput is close to the maximum near cell centre, and gradually descends for longer distances (while UE approaches the cell edge). This decrease is more evident for NLoS propagation. Although the comparison of the behaviour between bandwidths of 10 and 20 MHz is not presented in these charts, the wider bandwidth is the lower is CNIR. From the results, this evidence is clearer for NLoS propagation but only slightly noticed for LoS propagation, as  $N \ll I$  and interference becomes dominant. Figure 10 analyses the equivalent supported throughput,  $R_{b-sup}$ , as a function of  $R$ , for pico/macro cells with sizes up to 300 and 3000 m, respectively.

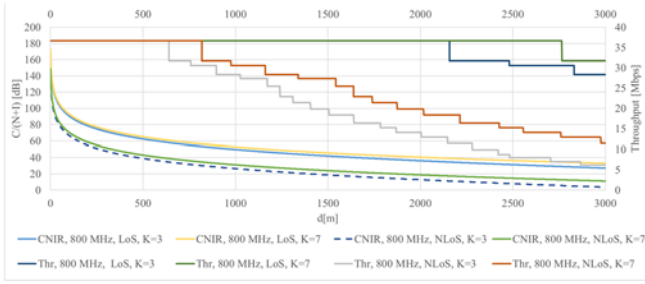


Fig. 8 Comparison of CNIR and  $R_b$  between  $K=7$  and 3 for the macro cellular scenario ( $f=800$  MHz),  $BW=10$  MHz, and LoS versus NLoS.

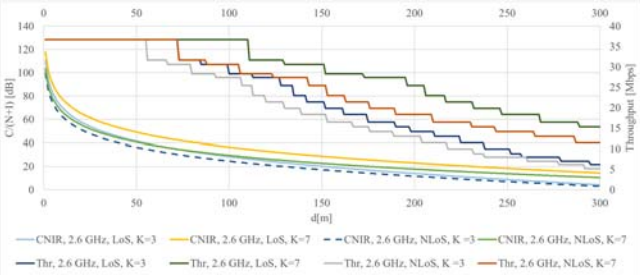


Fig. 9 Comparison of CNIR and  $R_b$  between  $K=7$  and 3 for the pico cellular scenario ( $f=2.6$  GHz),  $BW=10$  MHz, and LoS versus NLoS.

$R_{b-sup}$  is determined through a weighted sum of the PHY throughput in each coverage ring throughout the cell, where the weights are the individual areas of each of the coverage rings. Bandwidth is 10 MHz.  $R_{b-sup}$  is clearly superior for  $K=7$  and lower for  $K=3$ . The curves for macro cellular scenario (blue and green continuous curves) show that for LoS case,  $R_{b-sup}$  has a maximum constant behaviour for  $R>185$  and  $R>75$  ( $K=3$ ,  $K=7$ ). In the NLoS case, the curves show the same behaviour for  $K=3$  and  $K=7$ .  $R_{b-sup}$  starts decreasing after  $\sim 875$ m. The curves for pico cellular scenario are the dashed ones. At 2.6 GHz, for the NLoS model, the  $R_{b-sup}$  starts decreasing at  $R>70$  m for  $K=7$  and  $R>95$  m for  $K=3$ . For 2.6 GHz, LoS,  $R_{b-sup}$  starts increasing when the values of  $R$  reach  $R_0 = d_{BP}/r_{cc}$ , i.e.,  $R_0=52$  m for  $K=3$  and  $R_0=34$  m for  $K=7$ . For 2.6 GHz, LoS, there is a continuous behaviour with a maximum  $R_{b-sup}$  that occurs for the largest  $R_s$  ( $R>225$  m for  $K=3$  and  $R>75$  m for  $K=7$ ). For  $R<d_{BP}/r_{cc}$  the propagation exponents considered in the computation of  $C(R)=P_R(R)$  and  $I$  are the same ( $\gamma=2.2$ ), while for  $R_0 \leq R \leq 156$  m the propagation exponent to compute  $I$  is 4 (for interferers at distance  $D+d$ ) and 2.2 (for interferers for the rest of interferers), and the coverage is still computed with  $\gamma=2.2$ .

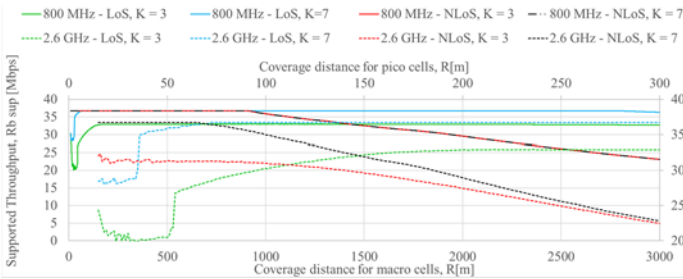


Fig. 10 Comparison of the equivalent supported throughput between  $K=7$  and 3 for the pico/macro cellular scenarios and LoS/NLoS,  $BW=10$  MHz.

Hence, because of the resulting less interference in this range of  $R_s>R_0$ , a significant increase into the maximum achievable  $R_{b-sup}$  is achieved, facilitating the optimization of SC networks. Macro and pico cells can obtain the same maximum achievable  $R_{b-sup}$ .

This analysis gives very useful hints for the optimization of CA [5], [7] between macro and pico cellular layer of a LTE-A HetNet with outdoor pico cells as trade-offs associated with the use different  $K_s$  are highlighted for LoS/NLoS propagation conditions.

#### IV. CONCLUSION

For cellular radio and network optimization purposes, the UL and DL carrier-to-noise-plus-interference ratios (CNIRs) from/at the mobile station are very important parameters. From a detailed analysis of its variation with the coverage and reuse distances for different LTE-A system parameters, modulation and coding schemes, in the DL, and ITU-R propagation models, an evaluation of the possible range for the reuse pattern has been performed. By considering the MCS and reference CNIR requirements recommended by 3GPP, DL peak bit rates along with the Transport Block Size assumed for single stream and bandwidths of 10 MHz and 20 MHz, an analysis of the physical and supported throughputs has been performed. One can learn that one common characteristic of the two frequency bands with NLoS propagation is the initial constant value for the  $R_{b-sup}$  followed by a clear decrease of the supported throughput with the coverage distance,  $R$ . Besides, for the small cell layer, operating at 2.6 GHz, owing to the behaviour of the two slope model in LoS propagation conditions, a clear increase in  $R_{b-sup}$  occurs for system capacity for  $R_s$  superior to  $d_{BP}/r_{cc}$ , after which it achieves a constant maximum in the range of  $R_s$  up to 300 m. Results show that picocells operating at 2.6 GHz should have cell coverage superior to  $d_{BP}/r_{cc}$ . The same maximum value is achieved for  $R_{b-sup}$  by pico and macro cells for the considered  $R_s$ . For the NLoS case, in the considered range of coverage distances, the clear decrease of  $R_{b-sup}$  does not occur for pico cells as for macro cells. However, the minimum values for the achieved  $R_{b-sup}$  are coincident both for  $K=3$  and  $K=7$ .

#### ACKNOWLEDGMENT

This work has been partially supported and funded by CREaTION, COST CA 15104, ECOOP, UID/EEA/50008/2013, EFATraS, SFRH/BSAB/113798/2015 and ORCIP.

#### REFERENCES

- [1] Cisco Visual Networking Index: Global Mobile Data Traffic Forecast Update, 2013-2018, white paper, Feb. 2014.
- [2] N. K. Noordin, B. M. Ali, N. Ismail, S. S. Januar, "Adaptive techniques in orthogonal frequency division multiplexing in mobile radio environment, *International Journal of Engineering and Technology*, vol. 1, no. 2, 2004.
- [3] 3GPP, TS 36.212, V11.3.0. Technical Specification Group Radio Access Network; Evolved Universal Terrestrial Radio Access (E-UTRA); Multiplexing and channel coding, 3GPP Std., June 2013.
- [4] 3GPP Ts 36.300, V10.8.0 Rel. 10 Evolved Universal Terrestrial Radio Access (E-UTRA) and Evolved Universal Terrestrial Radio Access Network (E-UTRAN); Overall description; Stage 2, July 2012.
- [5] Jessica Acevedo, Daniel Robalo, Fernando J. Velez, "Transmitted Power Formulation for the Optimization of Spectrum Aggregation in LTE-A over 800 MHz and 2 GHz Frequency Bands," *Wireless Pers. Comms.*, June 2015.
- [6] Guidelines for evaluation of radio interface technologies for IMT-Advanced, Report ITU-R M.2135-1, Dec. 2009.
- [7] Daniel Robalo, *Planning and Dynamic Spectrum Management in Heterogeneous Mobile Networks with QoE Optimization*, Ph.D. thesis, Universidade da Beira Interior, Covilhã, Portugal, 2014.